Finite time singularities against observations

Tomasz Denkiewicz

Section of Cosmology and Gravitation Theory

Institute of Physics

Faculty of Mathematics and Physics

Szczecin University

Copernicus Center for Interdisciplinary Studies, Kraków, Poland

27.IV.15 - 01.V.15 Cargèse

Overview

Singularities

Singularities vs observations

Varying α with singularities

Conclusions

Singularities

Finite time singularities

- Type I (“Big Rip”) : For $t \to t_s$, $a \to \infty$, $\rho \to \infty$ and $|p| \to \infty$ R.R. Caldwell, M. Kamionkowski, and N.N. Weinberg, Phys. Rev. Lett. **91**, 071301 (2003);
- Type II (“sudden”) : For $t \to t_s$, $a \to a_s$, $\rho \to \rho_s$ and $|p| \to \infty$ J.D. Barrow and Ch. Tsagas, Class. Quantum Grav. **22**, 1563 (2005);
- Type III (“FSF”) : For $t \to t_s$, $a \to a_s$, $\rho \to \infty$ and $|p| \to \infty$
- Type IV : For $t \to t_s$, $a \to a_s$, $\rho \to 0$, $|p| \to 0$ and higher derivatives of H diverge.
- w-singularities: For $t \to t_s$, $|p| \to 0$, $\rho \to 0$, $q \to \infty$ & $w \to \infty$ M.P. Dąbrowski & TD, Physical Review D 79, 063521 (2009);
- little-rip, pseudo-rip, quasi-rip

Here t_s, a_s and ρ_s are constants with $a_s \neq 0$.

Nojiri, Shin’ichi, Odintsov, Sergei D., and Tsujikawa, Shinji:
Properties of singularities in the (phantom) dark energy universe,
Physical Review **D71** 063004, (2005);

Finite time singularities within physical models

- w-singularity
  - $f(R)$ – gravity A. A. Starobinsky, Phys. Lett. 91B, 99 (1980)
  - scalar field models M. R. Setare and E. N. Saridakis, Phys. Lett. B671, 331 (2009)
  - brane cosmologies V. Sahni and Yu. Shtanov, Phys. Rev. D 71, 084018 (2005)
- Type II - SFS
  - cosmological models based on the loop quantum gravity T. Cailleteau, A. Cardoso, K. Vandersloot, and D. Wands, Phys. Rev. Lett. 101, 251302 (2008)
  - some of dark energy EOS Shin'ichi Nojiri, Sergei D. Odintsov, and Shinji Tsujikawa Phys. Rev. D 71, 063004 (2005)

Scale factor parametrization

- $a(t) = a_s \left[1 + (1-\delta)\, y^m - \delta\, (1-y)^n\right]\ , \qquad y \equiv \frac{t}{t_s}$

  with the appropriate choice of the constants δ, t_s, a_s, m, n.

- $2 > n > 1$ - SFS pressure singularity $p \to -\infty$ occurs when the acceleration $\ddot{a} \to +\infty$, no matter that the value of the energy density ϱ and the scale factor $a(t)$ are regular.

- $1 > n > 0$ - Type III singularity, $\rho \to \infty$ and $|p| \to \infty$

Singularities vs observations

Supernovae Ia

The luminosity distance to supernova is given by

$$d_L(z) = (1+z)ct_s \int_{y_1}^{y_0} \frac{dy}{a(y)} \qquad (1)$$

and the distance modulus is

$$\mu(z) = 5\log_{10} d_L(z) + 25. \qquad (2)$$

The χ^2 for the SNIa data is

$$\chi^2_{SN} = \sum_{i=1}^{N} \frac{(\mu_{obs}(z_i) - \mu(z_i))^2}{\sigma_i^2 + \sigma_{int}^2}, \qquad (3)$$

where σ_i is the quoted observational error on the i^{th} Union2 SNIa and σ_{int} is the SNIa intrinsic scatter.

Supernovae Ia - Type II/III

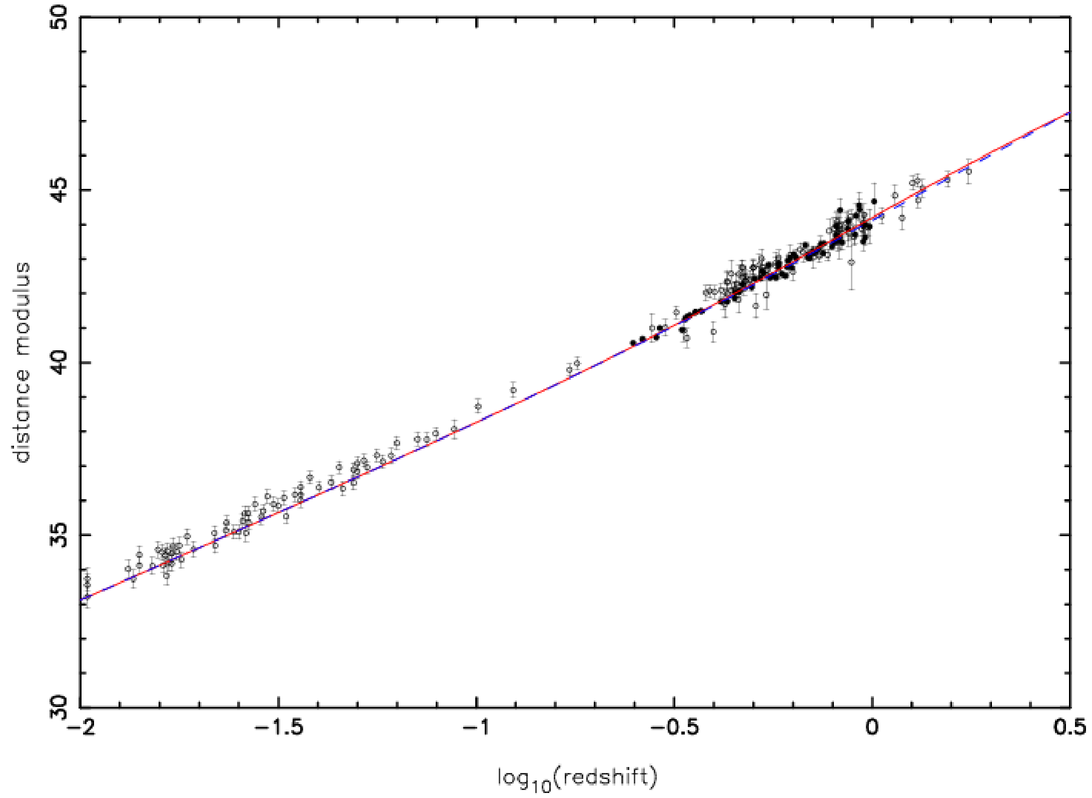

Figure 1: The distance modulus $\mu_L = m - M$ for the concordance cosmology (CC) model with $H_0 = 72 \text{kms}^{-1}\text{Mpc}^{-1}$, $\Omega_{m0} = 0.26$, $\Omega_{\Lambda 0} = 0.74$ (dashed curve) and sudden future singularity (SFS) model for $m = 2/3, n = 1.9999, \delta = -0.471, y_0 = 0.99936$ (solid curve). Also shown are the 'Gold' (open circles) and SNLS (filled circles) SN Ia data. Taking the age of the SFS model to be equal to that of the CC model, i.e. $t_0 = 13.6$ Gyr, one finds that an SFS is possible in only 8.7 My.

M.P. Dąbrowski, TD, M.A. Hendry, *How far is it to a sudden future singularity of pressure?*, Physical Review D**75**, 123524 (2007)

Supernovae Ia - Type II/III

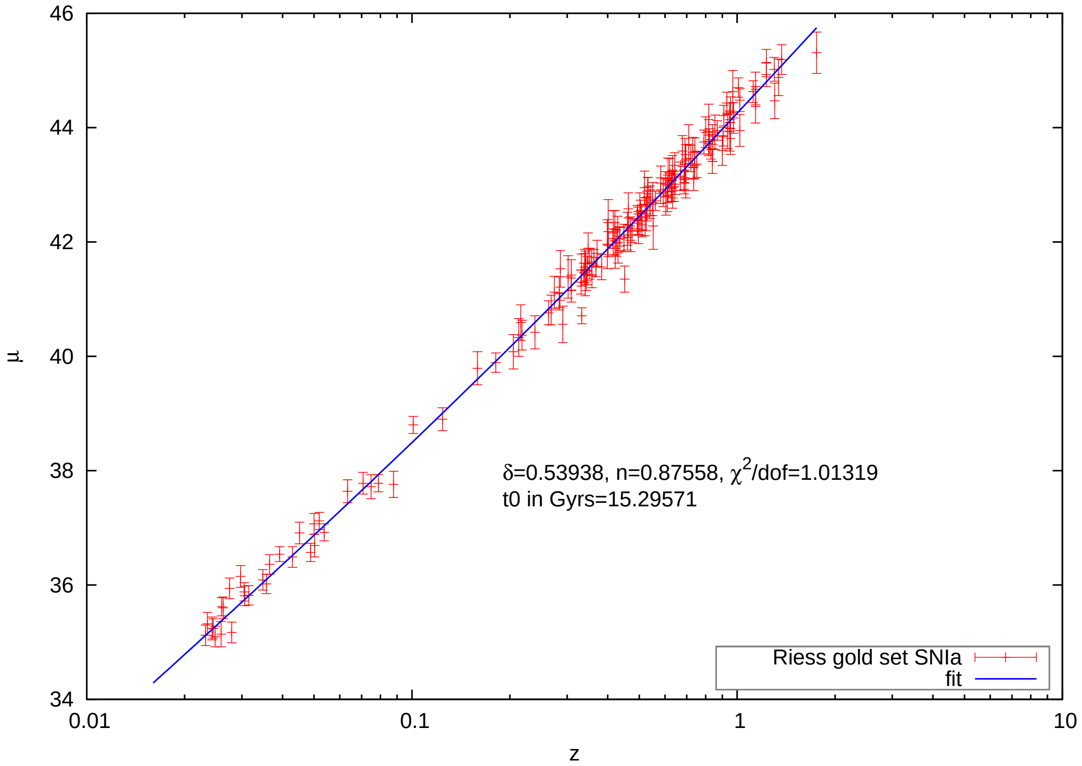

Figure 1: M.P. Dabrowski and T. Denkiewicz, AIP Conference Proceedings **1241**, 561 (2010); arXiv: 0910.0023

How hard is to fit the data

With four parameters I can fit an elephant, and with five I can make him wiggle his trunk.

John von Neumann(28 December 1903 – 8 February 1957) was a Hungarian-American-German-Jewish mathematician and computer scientist, generally regarded as one of the foremost mathematicians of the 20th century.

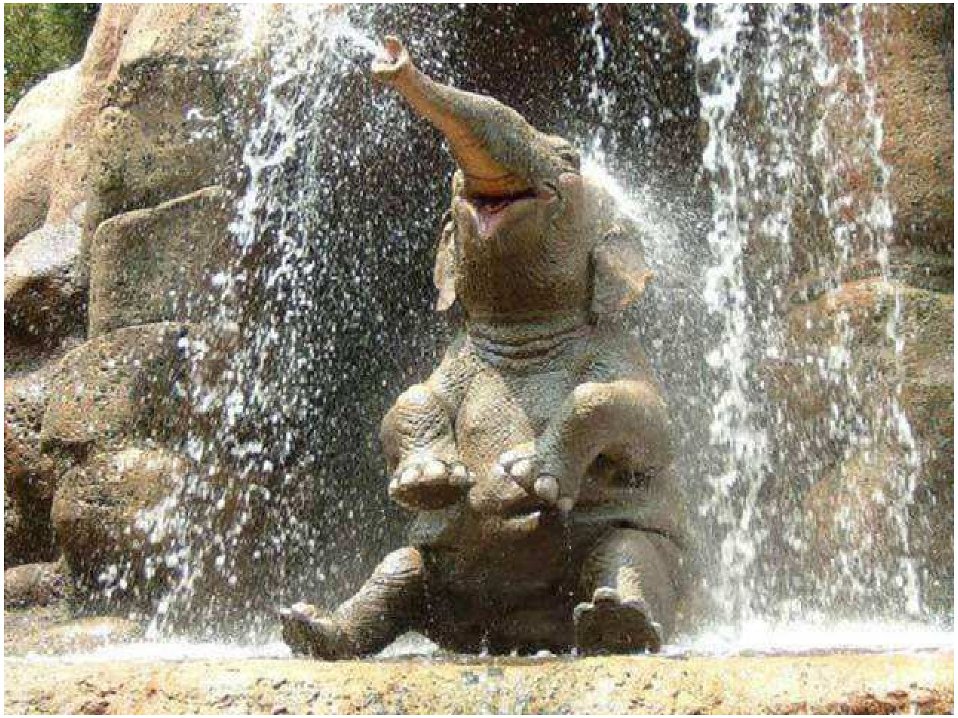

How hard is to fit the data

With four parameters I can fit an elephant, and with five I can make him wiggle his trunk.

John von Neumann(28 December 1903 – 8 February 1957) was a Hungarian-American-German-Jewish mathematician and computer scientist, generally regarded as one of the foremost mathematicians of the 20th century.

Shift parameter

The shift parameter is

TD, M. P. Dabrowski, H. Ghodsi, M. A. Hendry, Phys.Rev. D85 (2012) 083527;

$$\mathcal{R} = \sqrt{\Omega_{m0}} a'(y_0) \int_{y_1}^{y_0} \frac{dy}{a(y)}, \tag{4}$$

where $'$ denotes derivative with respect to y. The WMAP data gives $\mathcal{R} = 1.725 \pm 0.018$,

N. Jarosik et al., The Astroph. J. Supplement Series, **192**, 2 (2011)

thus χ^2 for the shift parameter is the following

$$\chi^2_R = \frac{(\mathcal{R} - 1.725)^2}{0.018^2} \tag{5}$$

Baryon acoustic oscillations

$$\mathcal{A} = \Omega_{0m}^{1/2} E(z_{BAO})^{-1/3} \left[\frac{1}{z_{BAO}} \int_0^{z_1} \frac{dz'}{E(z')} \right]^{2/3} \tag{6}$$

$$\mathcal{A} = \Omega_{0m}^{1/2} a'(y_0) \left[\frac{a(y_{bao})}{a'(y_{bao}) a(y_0)} \right]^{\frac{1}{3}} \left[\frac{1}{z_{bao}} \int_{y_{bao}}^{y_0} \frac{dy}{a(y)} \right] \tag{7}$$

$$\chi_A^2 = \frac{(\mathcal{A} - 0.469)^2}{0.017^2} \tag{8}$$

TD, M. P. Dabrowski, H. Ghodsi, M. A. Hendry, Phys.Rev. D85 (2012) 083527;

Overall χ^2

$$\chi^2 = \chi_{SN}^2 + \chi_R^2 + \chi_A^2 \tag{9}$$

Results

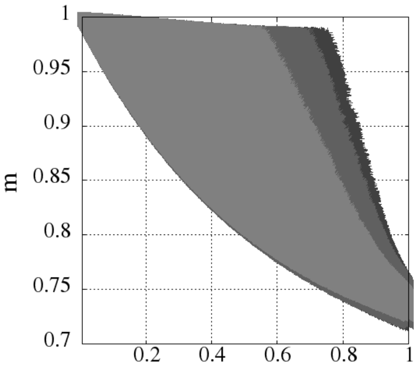

Marginalized contours for pairs of parameters are plotted. There are three confidence regions 68%, 95%, 99% (from light grey to dark grey respectively) calculated from $\mathcal{A}$, $\mathcal{R}$, and SN Ia jointly.

H. Ghodsi, M. A. Hendry, M. P. Dabrowski, TD, MNRAS, 414: 15171525 (2011);

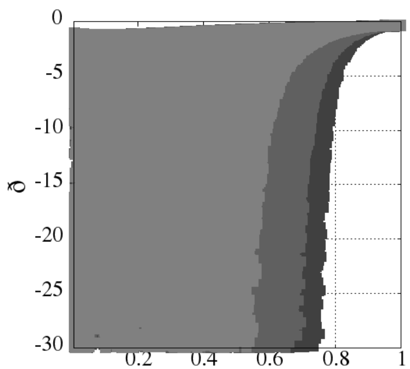

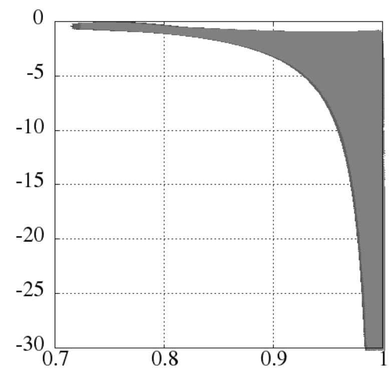

TD, M. P. Dabrowski, H. Ghodsi, M. A. Hendry, Phys.Rev. **D85** (2012) 083527;

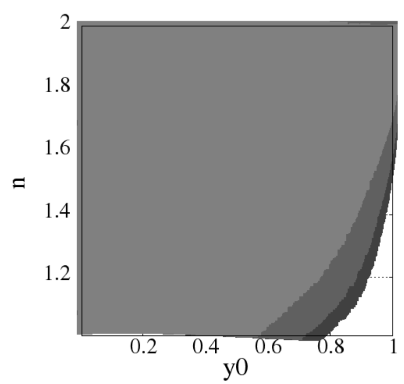

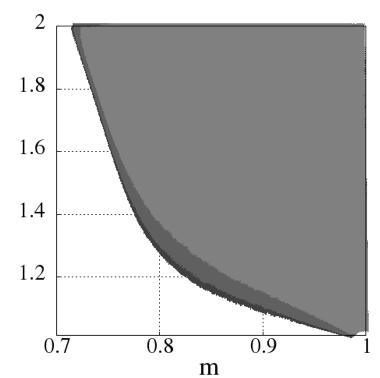

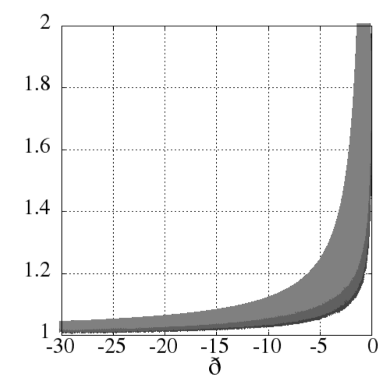

Results

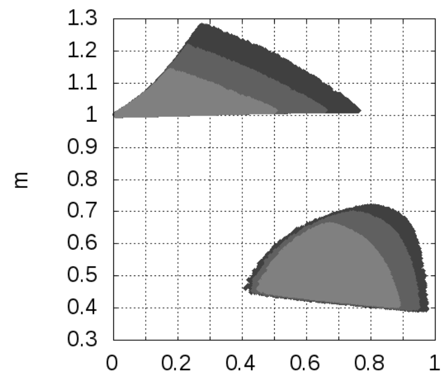

Marginalized contours for pairs of parameters are plotted. There are three confidence regions 68%, 95%, 99% (from light grey to dark grey respectively) calculated from $\mathcal{A}$, $\mathcal{R}$, and SN Ia jointly.

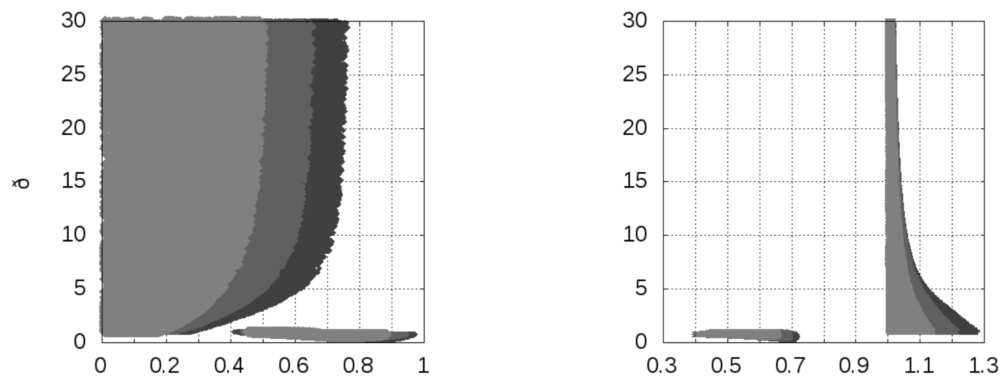

TD, Observational Constraints on Finite Scale Factor Singularities, [arXiv:1112.5447]; JCAP 1207 (2012) 036

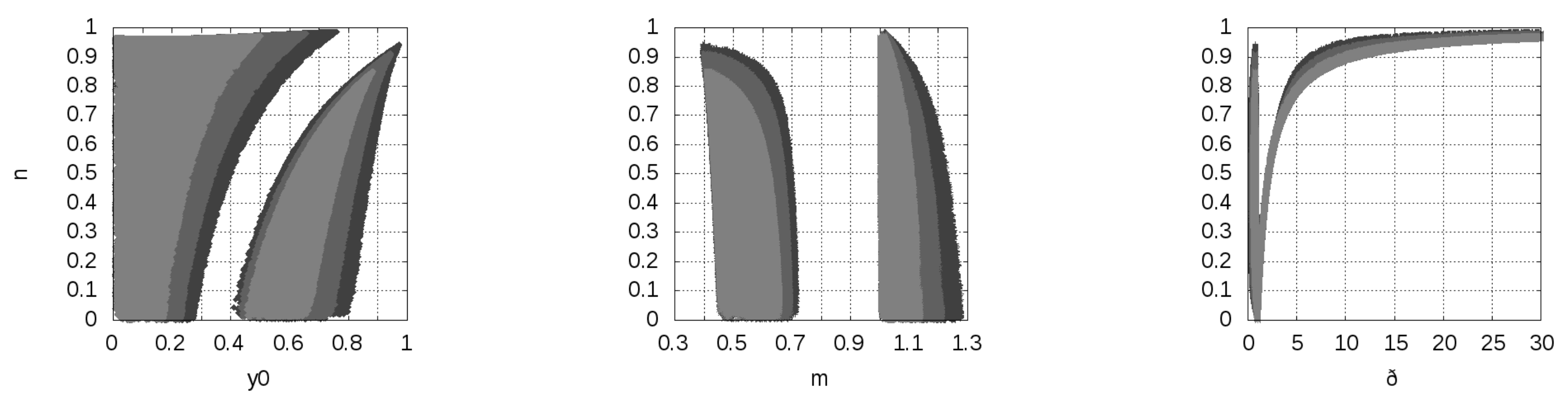

Matter density fluctuations

- Evolution of density perturbations in cosmological models which admit finite scale factor singularities.
- After solving the matter perturbations equations we find that there exists a set of the parameters which admit a finite scale factor singularity in future and instantaneously recover matter density evolution history which are indistinguishable from the standard ΛCDM scenario.

Matter density fluctuations

In the linear regime the equations that govern the evolution of perturbations in a Friedmann universe consisting of more than one component constitute a complicated set of coupled differential equations [1]. We consider the evolution of perturbations in a flat Friedmann universe made up of a dust matter with the density ρ_m and a dark energy with density ρ_{de}, and pressure p_{de}. It was shown in [2] that, in similar case, neglecting perturbations in dark energy one makes some particular, unintended choice of gauge and in general that may lead to errorneous results for perturbations in the matter. Taking that into account **we restrict our investigations to the cases where the proper wavelength of perturbations is much smaller than the Hubble radius and the sound velocity for the dark energy has a positive value of order of unity, while the barotropic index for the dark energy is a reasonable slowly varying function of the cosmic time.**

---

[1] Mukhanov V F, Feldman H A and Brandenberger R H, *Theory of cosmological perturbation*, 1992 *Phys. Rep.* **215** 205;

[2] A. J. Christopherson Phys. Rev. D82, 083515 (2010);

Matter density fluctuations

With these assumptions the dark matter perturbations effectively decouple from perturbations in the dark energy and the evolution of the matter density contrast δ_m can be described to a good approximation with the following equations:

$$\ddot{\delta}_m + 2H\dot{\delta}_m = 4\pi G \rho_m \delta_m, \tag{10}$$

$$\left(\frac{\dot{a}}{a}\right)^2 = \frac{8\pi G}{3}(\varrho_m + \varrho_{de}) \tag{11}$$

$$2\frac{\ddot{a}}{a} + \left(\frac{\dot{a}}{a}\right)^2 = -8\pi G p_{de}, \tag{12}$$

where a dot denotes a derivative with respect to time $H = \dot{a}/a$ is the Hubble parameter.

$$\ddot{\delta} + 2\frac{\dot{a}}{a}\dot{\delta} = 4\pi\rho_m\delta \tag{13}$$

$$\Omega_m(y) = H_{y0}^2\omega_m\frac{aa_{y0}^3}{\dot{a}^2} \tag{14}$$

$$\dot{f}\frac{a}{\dot{a}} + f^2 + f\left(\frac{\ddot{a}a}{\dot{a}^2} + 1\right) - \frac{3}{2}\Omega_m(y) = 0 \tag{15}$$

$$f \equiv \frac{d\ln\delta}{d\ln a} \tag{16}$$

z	f_{obs}
0.15	0.51 ± 0.11
0.35	0.7 ± 0.18
0.55	0.75 ± 0.18
1.4	0.9 ± 0.24
3.0	1.46 ± 0.29

Table 1: Observational data for the growth factor f from Lyman-α forests and galaxy redshift distortions taken from Refs:

L. Guzzo et al., Nature 451, 541 (2008); M. Colless et al., Mont. Not. R. Astron. Soc. 328, 1039 (2001); M. Tegmark el al., Phys. Rev. D 74, 123507 (2006); N.P. Ross et al., Mont. Not. R. Astron. Soc. 381, 573 (2007); J. da Angela ˆ et al., Mont. Not. R. Astron. Soc. 383, 565 (2008); P. McDonald et al., Astrophys. J. 635, 761 (2005);

We solve the equation for density evolution numerically for a given set of the parameters using the standard Runge-Kutta method with an adaptative step size. Applying a standard Levenberg-Marquardt method, we search for the minimum of the χ^2 function which is of the form

$$\chi^2(z;\mathbf{p}) = \sum_{i=1}^{5} \frac{(f_{obs}(z_i;\mathbf{p}) - f_{th}(z_i;\mathbf{p}))^2}{\sigma_i^2}, \qquad (13)$$

where: f_{obs} and σ_i are taken from the table 1; f_{th} is calculated by solving the equation for f; $\mathbf{p} \equiv (m, n, \delta, y_0, f_0)$. We find the following fit for one of the possible set of parameters:

$$y_0 = 0.55,\ \delta = 0.67,\ m = 0.49,\ n = 0.32,\ f_0 = 0.53, \qquad (14)$$

with $\chi^2 = 0.99$.

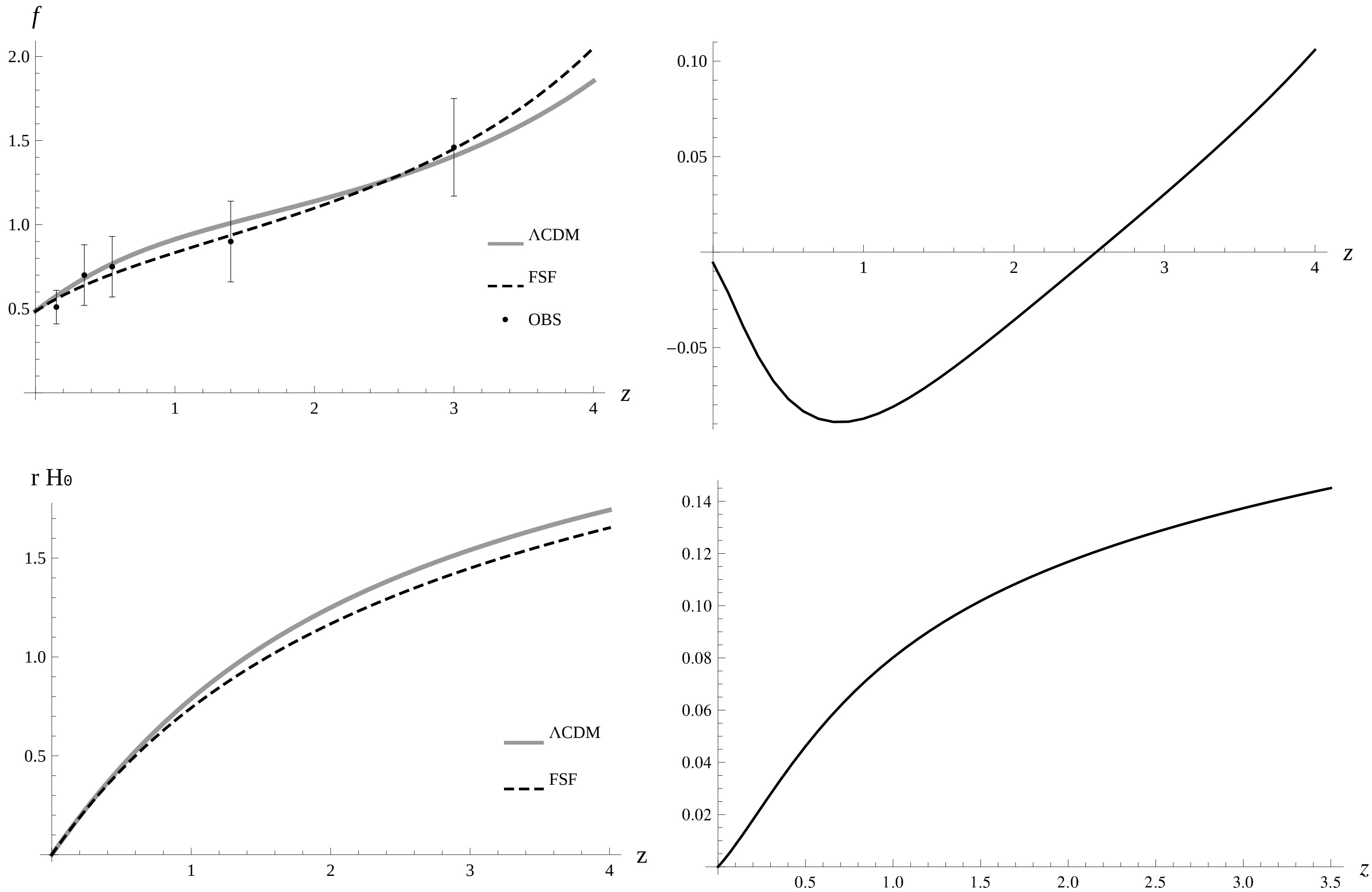

Upper left panel presents the predicted growth rate plotted against redshift for an FSF model (dashed line) and a ΛCDM model (solid line). There are also shown the observed data points (dots) for the growth rate. The upper right panel shows the distance-redshift relation for both FSF and ΛCDM models. The left and right bottom panels present the corresponding relative errors.

A. Balcerzak, TD, Phys. Rev. D86 (2012) 023522, arXiv:1202.3280

$$\begin{cases} \Delta\Psi - 3\mathcal{H}\left(\mathcal{H}\Phi + \Psi'\right) + 3\mathcal{K}\Psi = a^2\delta\rho \\ \mathcal{H}\Phi + \Psi' = a\left(\rho + p\right)V \\ \left[\Psi'' + \mathcal{H}\Phi' + \left(2\mathcal{H}' + \mathcal{H}^2\right)\Phi + 2\mathcal{H}\Psi' - \mathcal{K}\Psi + \frac{1}{2}\Delta\left(\Phi - \Psi\right)\right]\delta^i_j - \\ -\frac{1}{2}\gamma^{ik}\left(\Phi - \Psi\right)_{|kj} = a^2\delta p\delta^i_j - \sigma^{|i}_{|j}, \end{cases} \tag{13}$$

Mukhanov V F, Feldman H A and Brandenberger R H, *Theory of cosmological perturbation*, 1992 *Phys. Rep.* **215** 205

$$\begin{cases} -k^2\Phi - 3a\mathcal{H}^2\dot{\Phi} - 3\mathcal{H}^2\Phi = a^2\sum_{i=1}^{N}\rho_i\delta_i \\ \mathcal{H}\Phi + a\mathcal{H}\dot{\Phi} = a\sum_{i=1}^{N}\left(\rho_i + p_i\right)V_i \\ \left(a\mathcal{H}\right)^2\ddot{\Phi} + \left(4a\mathcal{H}^2 + a^2\mathcal{H}\dot{\mathcal{H}}\right)\dot{\Phi} + \left(2a\mathcal{H}\dot{\mathcal{H}} + \mathcal{H}^2\right)\Phi = a^2\sum_{i=1}^{N}c^2_{\mathrm{s}i}\rho_i\delta_i \end{cases} \tag{14}$$

$$\begin{aligned} \ddot{\delta}_{\mathrm{m}} + \left(\frac{\dot{a}}{a} - \frac{\ddot{a}}{a}\right)\dot{\delta}_{\mathrm{m}} + \frac{k^2}{a^2}c^2_{s\mathrm{m}}\delta_{\mathrm{m}} = \rho_{\mathrm{m}}\delta_{\mathrm{m}} + \rho_{\mathrm{de}}\delta_{\mathrm{de}}, \\ \ddot{\delta}_{\mathrm{de}} + \left(\frac{\dot{a}}{a} - \frac{\ddot{a}}{a}\right)\dot{\delta}_{\mathrm{de}} + \frac{k^2}{a^2}c^2_{s\mathrm{de}}\delta_{\mathrm{de}} = \rho_{\mathrm{m}}\delta_{\mathrm{m}} + \rho_{\mathrm{de}}\delta_{\mathrm{de}}, \end{aligned} \tag{15}$$

V. Gorini, A.Y. Kamenshchik, U. Moschella, O.F. Piattella and A.A. Starobinsky, *Gauge-invariant analysis of perturbations in Chaplygin gas unified models of dark matter and dark energy*, *JCAP* **02** (2008) 016

T. Denkiewicz, *Dark energy and dark matter perturbations in singular universes*, *JCAP* **03** (2015) 037

$$\varrho(t) = \frac{3}{2}\left(\frac{\dot{a}}{a}\right)^2 \tag{16}$$

$$p(t) = -\frac{1}{2}\left(2\frac{\ddot{a}}{a} + \frac{\dot{a}^2}{a^2}\right) \tag{17}$$

$$\rho_m = \Omega_{m0}\rho_0\left(\frac{a_0}{a}\right)^3 \tag{18}$$

$$\rho_{de} = \rho - \rho_m \tag{19}$$

$$\Omega_m = \frac{\rho_m}{\rho}, \quad \Omega_{de} = \frac{\rho_{de}}{\rho} \tag{20}$$

$$\Omega_{de} = 1 - \Omega_{m0}\frac{H_0^2}{H^2(t)}\left(\frac{a_0}{a(t)}\right)^3 = 1 - \Omega_m \tag{21}$$

$$w_{de} = p_{de}/\rho_{de} \tag{22}$$

DM & DE

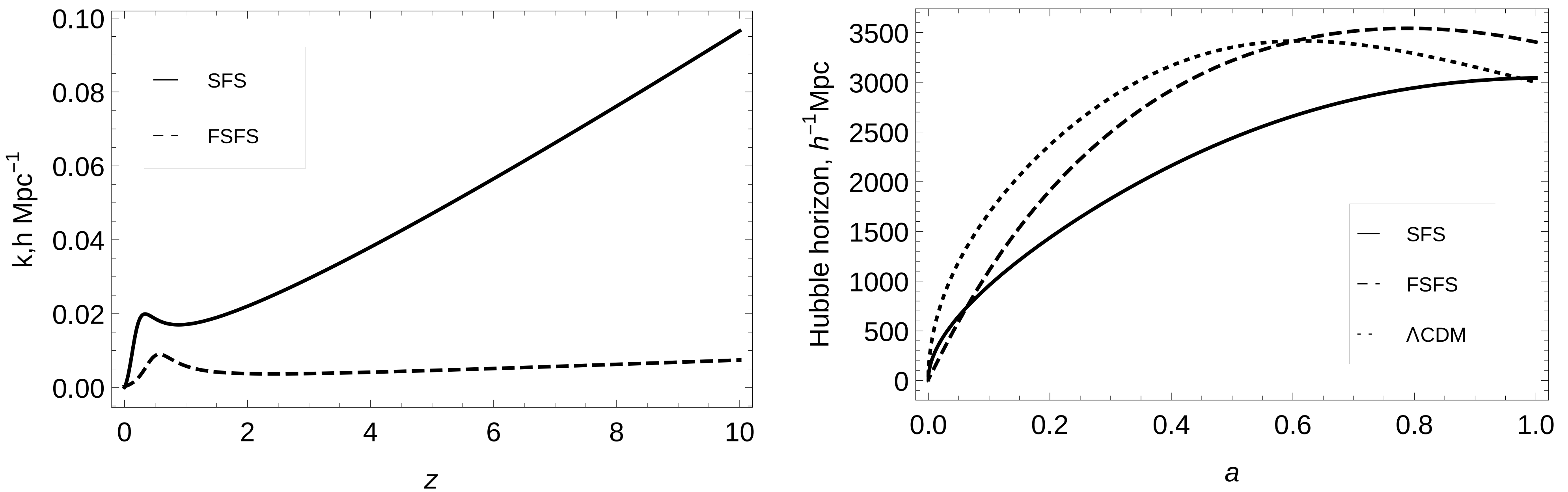

0.10
0.08
0.06
0.04
0.02
0.00
k,h Mpc^{-1}
SFS
FSFS
0
2
4
6
8
10
z
3500
3000
2500
2000
1500
1000
500
0
Hubble horizon, h^{-1}Mpc
SFS
FSFS
ΛCDM
0.0
0.2
0.4
0.6
0.8
1.0
a

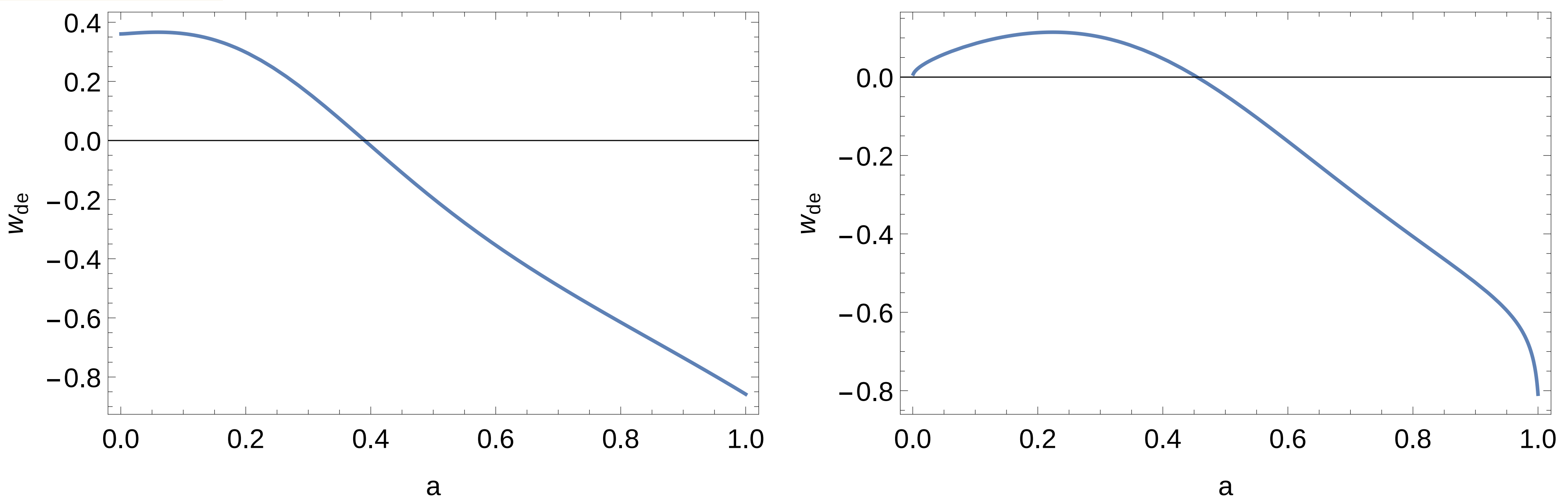

0.4
0.2
0.0
−0.2
−0.4
−0.6
−0.8
w_{de}
0.0
0.2
0.4
0.6
0.8
1.0
a
0.0
−0.2
−0.4
−0.6
−0.8
w_{de}
0.0
0.2
0.4
0.6
0.8
1.0
a

DM & DE

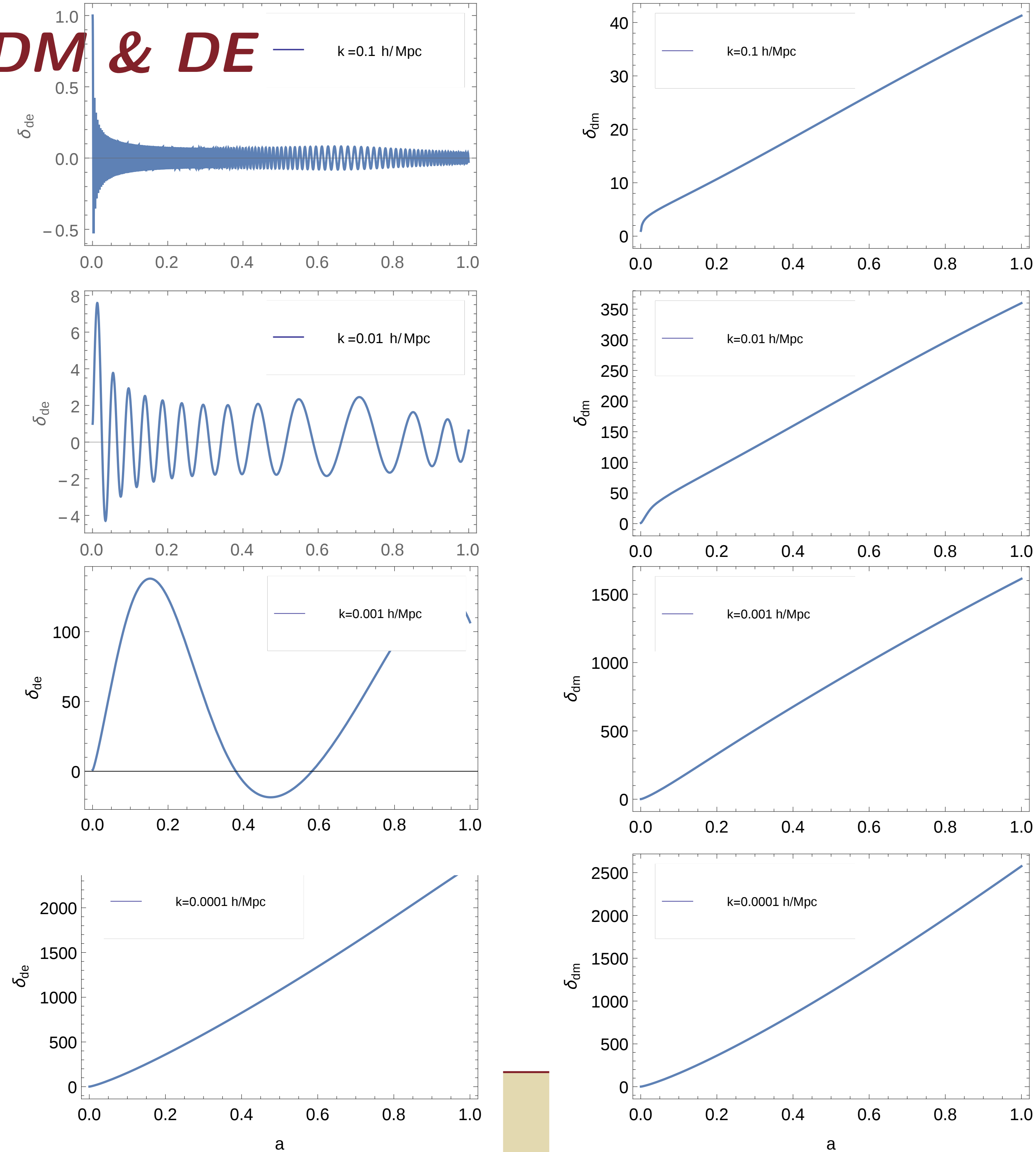
k =0.1 h/Mpc
δ_{de}
k=0.1 h/Mpc
δ_{dm}
k =0.01 h/Mpc
δ_{de}
k=0.01 h/Mpc
δ_{dm}
k=0.001 h/Mpc
δ_{de}
k=0.001 h/Mpc
δ_{dm}
k=0.0001 h/Mpc
δ_{de}
a
k=0.0001 h/Mpc
δ_{dm}
a

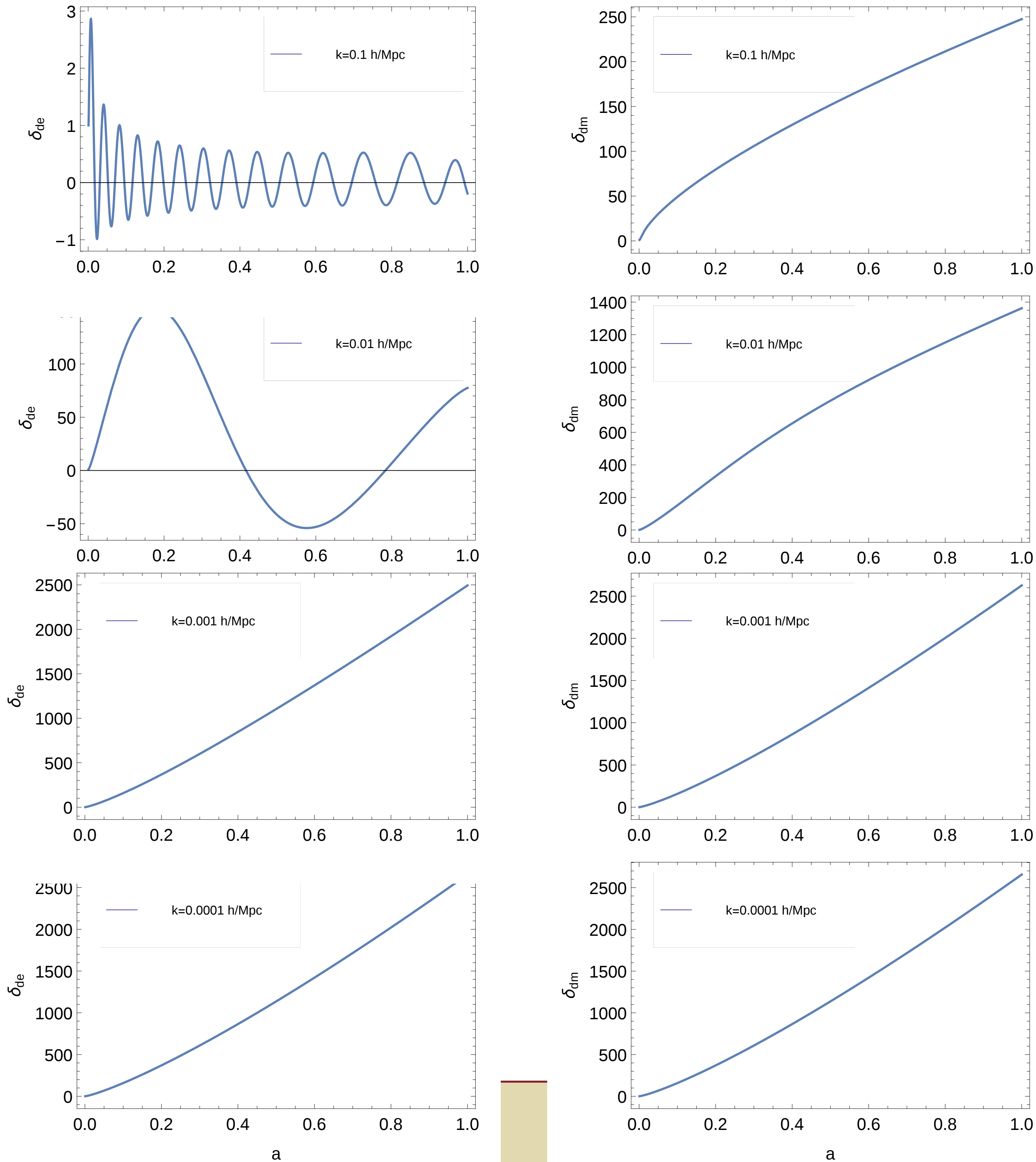
k=0.1 h/Mpc
δ_{de}
k=0.1 h/Mpc
δ_{dm}
k=0.01 h/Mpc
δ_{de}
k=0.01 h/Mpc
δ_{dm}
k=0.001 h/Mpc
δ_{de}
k=0.001 h/Mpc
δ_{dm}
k=0.0001 h/Mpc
δ_{de}
a
k=0.0001 h/Mpc
δ_{dm}
a

DM & DE

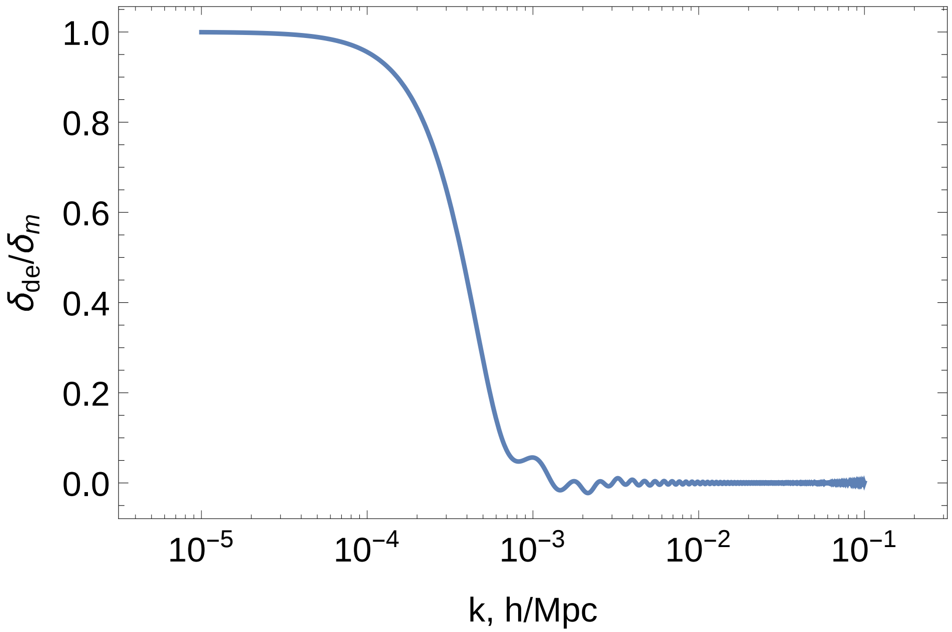

1.0
0.8
0.6
0.4
0.2
0.0
δ_{de}/δ_m
10^{-5} 10^{-4} 10^{-3} 10^{-2} 10^{-1}
k, h/Mpc

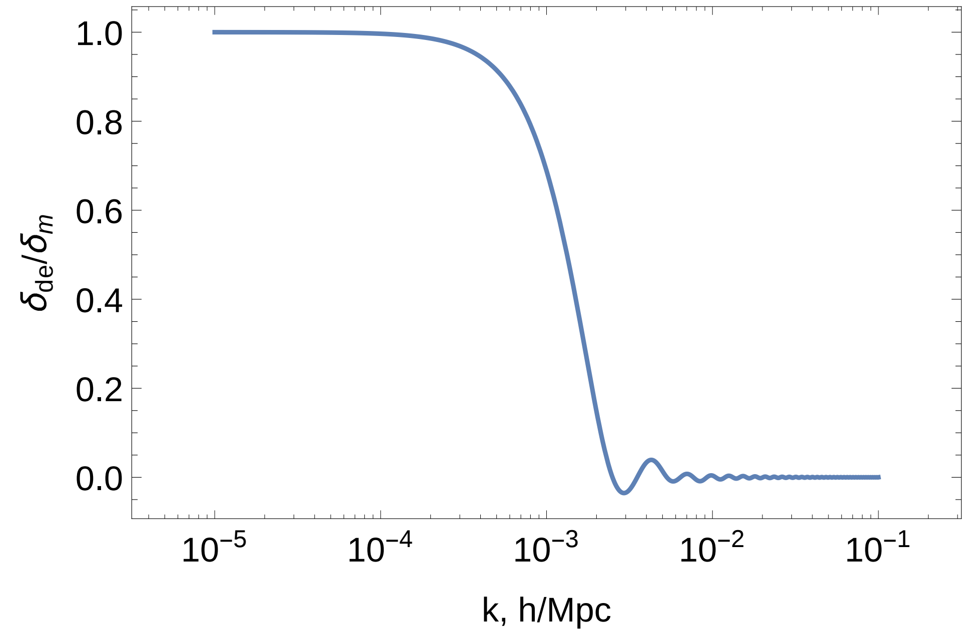

1.0
0.8
0.6
0.4
0.2
0.0
δ_{de}/δ_m
10^{-5} 10^{-4} 10^{-3} 10^{-2} 10^{-1}
k, h/Mpc

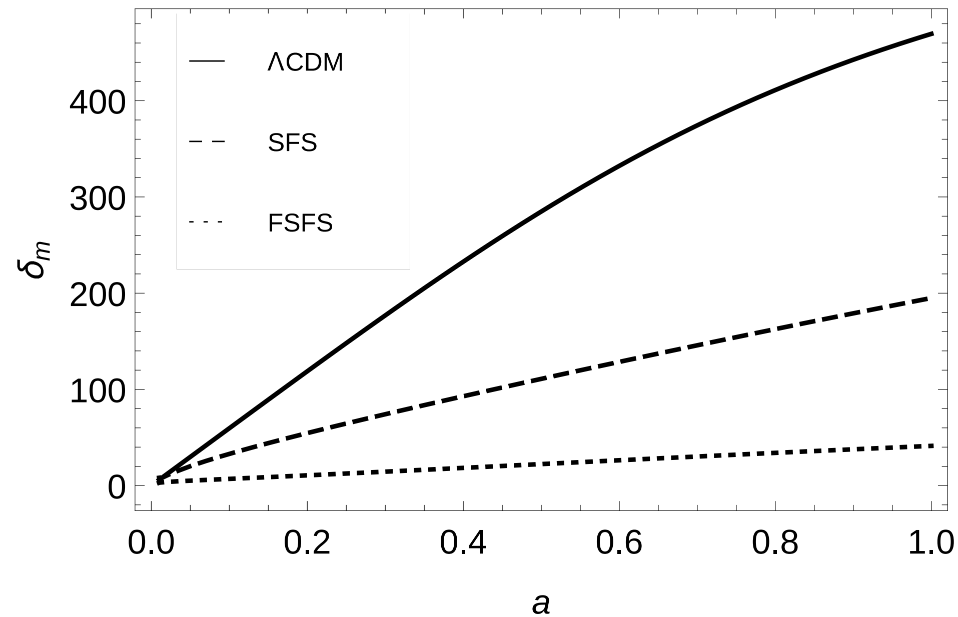

ΛCDM
SFS
FSFS
400
300
200
100
0
δ_m
0.0 0.2 0.4 0.6 0.8 1.0
a

Varying α with singularities

New measurements from QAS

- significant variations in α form high redsift quasar absorption line systems

$$\Delta\alpha/\alpha = (-0.573 \pm 0.113) \times 10^{-5}$$

- J.K. Webb, V.V.Flambaum, C.W. Churchill, et al., Phys. Rev. Lett **82**, 884 (1999)
- J.K. Webb, M.T. Murphy, V.V. Flambaum, et al., Phys. Rev. Lett **87**, 091301 (2001)
- Available specific measurements of α, with one-sigma uncertainties.

Object	Redshift	$\Delta\alpha/\alpha$	Spectrograph
HE0515-4414	1.15	$(-0.1 \pm 1.8) \times 10^{-6}$	UVES
HE0515-4414	1.15	$(0.5 \pm 2.4) \times 10^{-6}$	HARPS+UVES
HE0001-2340	1.58	$(-1.5 \pm 2.6) \times 10^{-6}$	UVES
HE2217-2818	1.69	$(1.3 \pm 2.6) \times 10^{-6}$	UVES
Q1101-264	1.84	$(5.7 \pm 2.7) \times 10^{-6}$	UVES

Quintessence

$$S = -\frac{1}{2\kappa}\int d^4x\sqrt{-g}R + \int d^4x\sqrt{-g}(\mathcal{L}_\phi + \mathcal{L}_M + \mathcal{L}_{\phi F}) \quad (23)$$

$$\mathcal{L}_\phi = \frac{1}{2}\partial^\mu\phi\partial_\mu\phi - V(\phi) \quad (24)$$

Coupling between the scalar field and electromagnetism

$$\mathcal{L}_{\phi F} = -\frac{1}{4}B_F(\phi)F_{\mu\nu}F^{\mu\nu}, \quad (25)$$

where

$$B_F(\phi) = 1 - \zeta\kappa(\phi - \phi_0)\,, \quad (26)$$

$\kappa^2 = 8\pi G$, ζ - constant. The evolution of α is given by

$$\frac{\Delta\alpha}{\alpha} \equiv \frac{\alpha - \alpha_0}{\alpha_0} = \zeta\kappa(\phi - \phi_0)\,, \quad (27)$$

Quintessence

Evolution of the scalar field in terms of the DE - Ω_ϕ and w:

$$w + 1 = \frac{(\kappa\phi')^2}{3\Omega_\phi}\,, \tag{23}$$

wherethe prime denotes the derivative with respect to $N = \ln a$.
The evolution of α:

$$\alpha/\alpha_0(a) = 1 - \zeta \int_a^{a_0} \sqrt{3\Omega_\phi(a)(1 + w(a))}d\ln a\,. \tag{24}$$

Quintessence

$$\Omega = \frac{\rho}{\rho_{cr}}, \quad \rho_{cr} = \frac{3H^2}{8\pi G} \tag{23}$$

$$\Omega_m = \Omega_{m0} \left(\frac{a_0}{a}\right)^3 \tag{24}$$

$$\Omega_\phi = \frac{\rho - \rho_m}{\rho_{cr}}, \tag{25}$$

$$\Omega_\phi = 1 - \Omega_{m0} \frac{H_0^2}{H} \left(\frac{a_0}{a}\right)^3 = 1 - \Omega_m \tag{26}$$

$$\alpha/\alpha_0(t) = 1 - \zeta \int_t^{t_0} \sqrt{3\Omega_\phi(t)(1 + w(t))} \frac{\dot{a}(t)}{a(t)} \, \mathrm{dt} \tag{27}$$

SFS

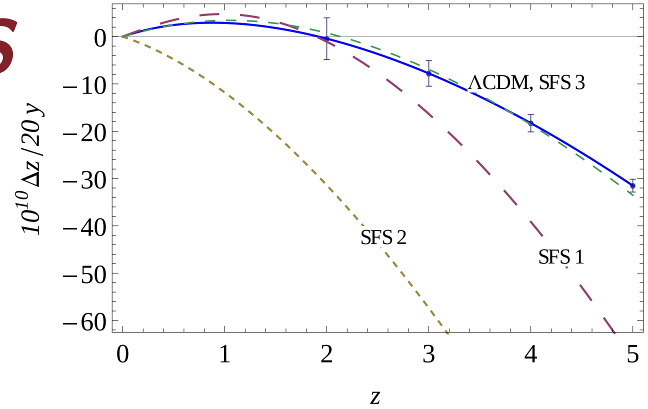

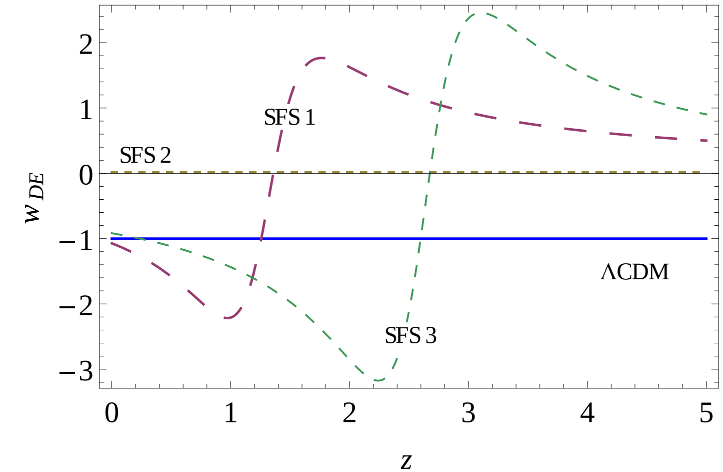

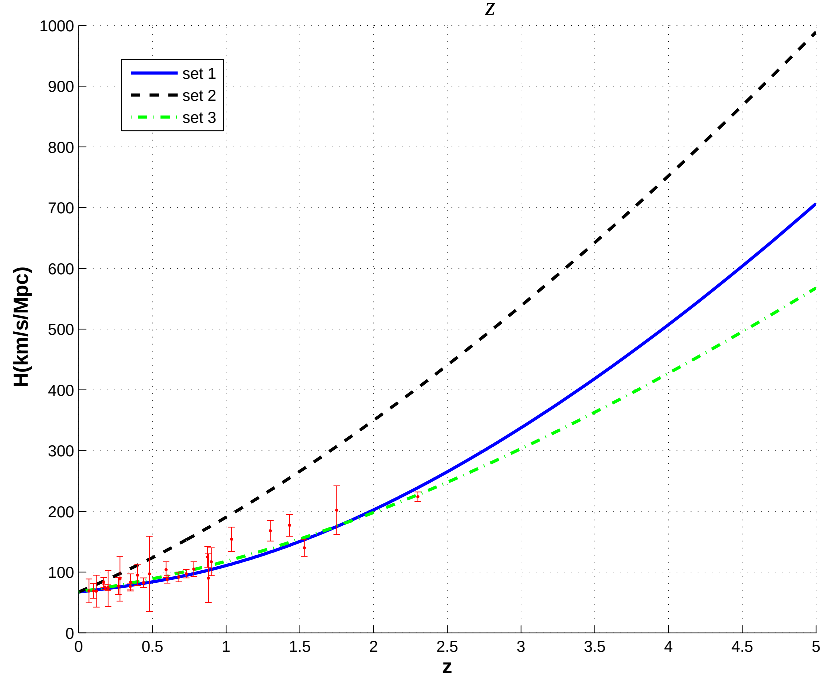

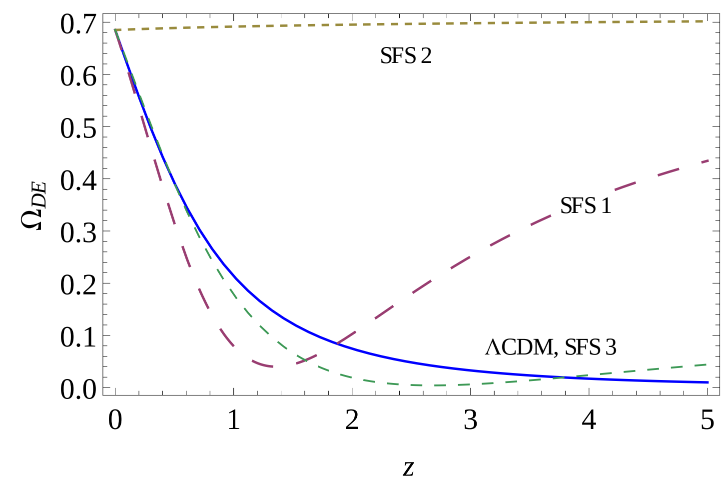

Model	m	n	δ	y_0
SFS1	2/3	1.9999	-0.43	0.99
SFS2	2/3	1.9999	0	0.99
SFS3	0.749	1.99	-0.45	0.77

M.P. Dabrowski, TD, CJAP Martins, P. E. Vielzeuf, arXiv:1406.1007, *Phys. Rev.* D 89, 123512
TD, M.P. Dabrowski, CJAP Martins, P. E. Vielzeuf, arXiv:1402.0520, *Phys. Rev.* D 89, 083514

SFS

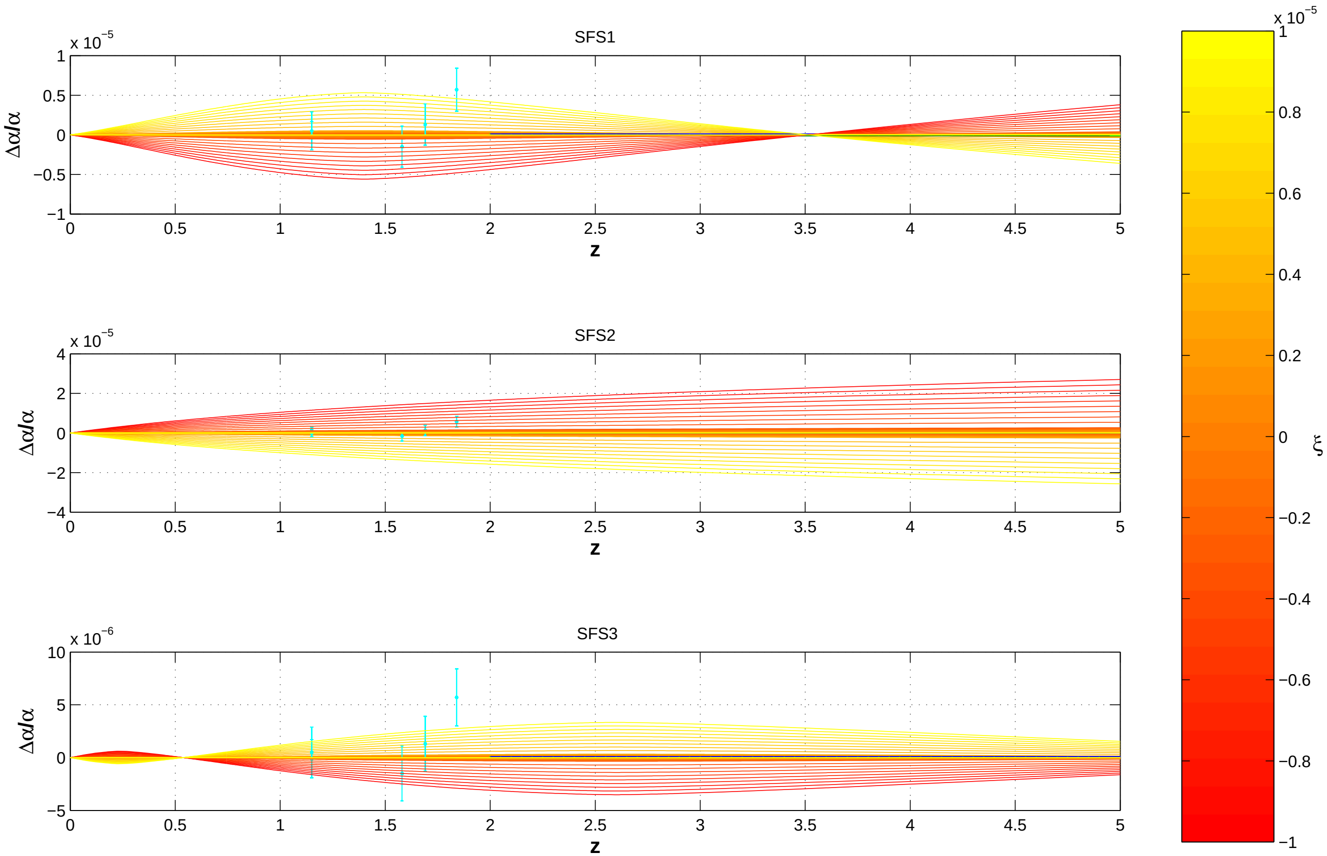

SFS1
x 10^{-5}
$\Delta\alpha/\alpha$
z
SFS2
x 10^{-5}
$\Delta\alpha/\alpha$
z
SFS3
x 10^{-6}
$\Delta\alpha/\alpha$
z
x 10^{-5}
ξ

SFS

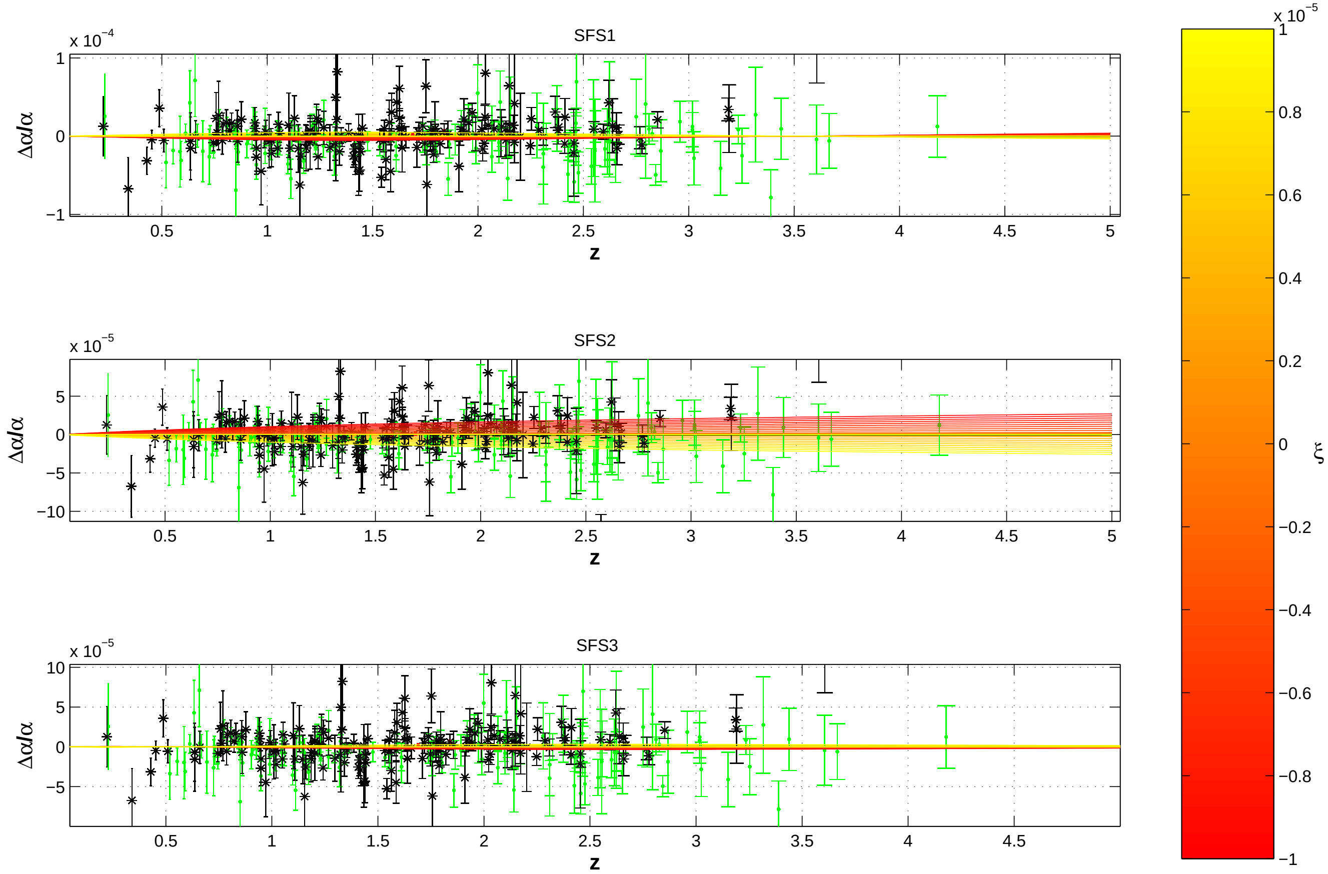

FSFS

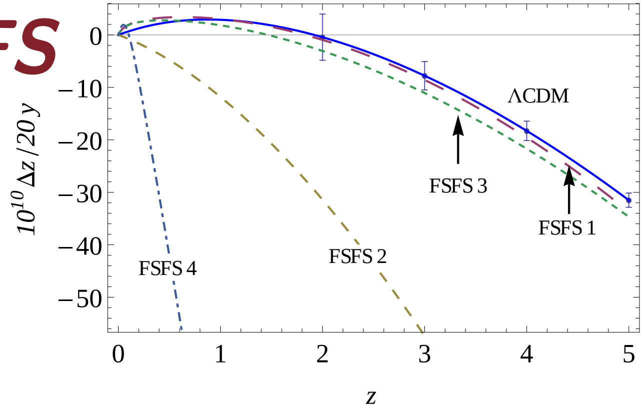

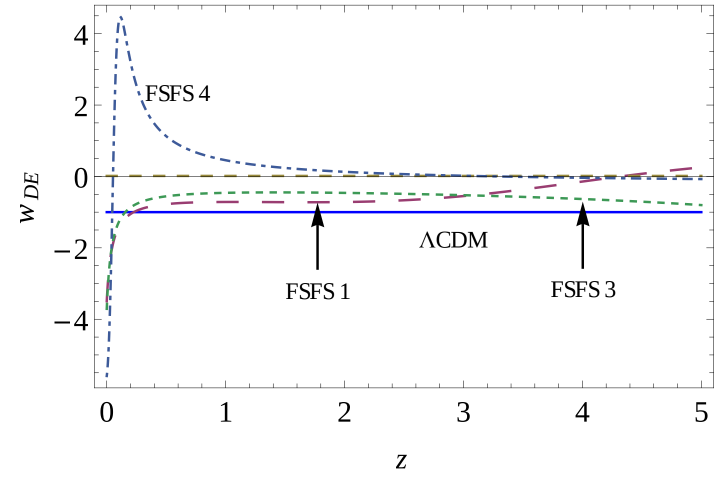

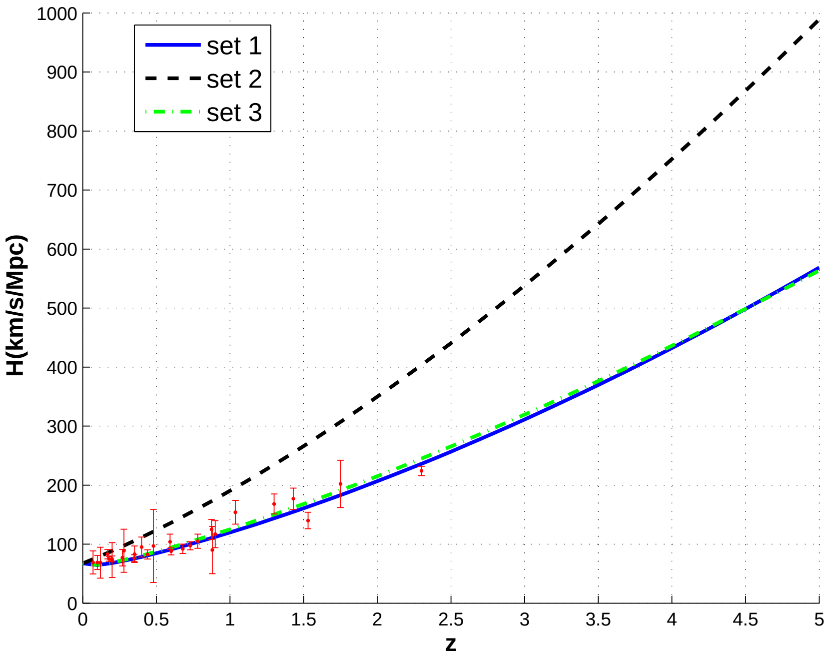

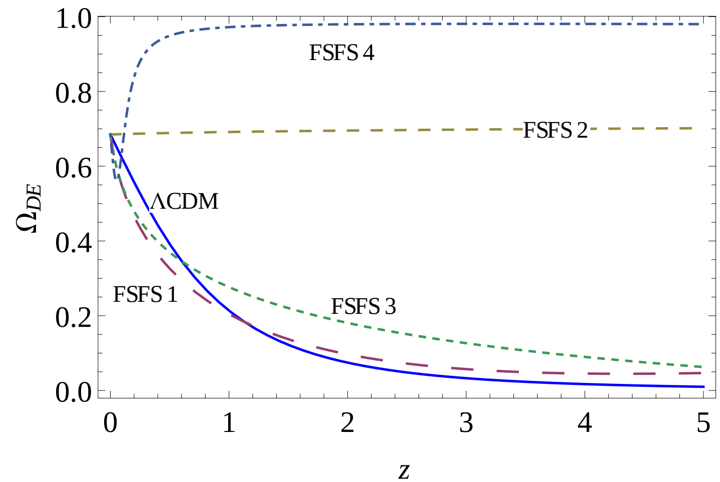

Model	m	n	δ	y_0
FSFS1	0.56	0.8	0.45	0.96
FSFS2	2/3	0.7	0	0.79
FSFS3	2/3	0.7	0.24	0.96

TD, M.P. Dabrowski, CJAP Martins, P. E. Vielzeuf, arXiv:1402.0520, *Phys. Rev.* D 89, 083514

FSFS

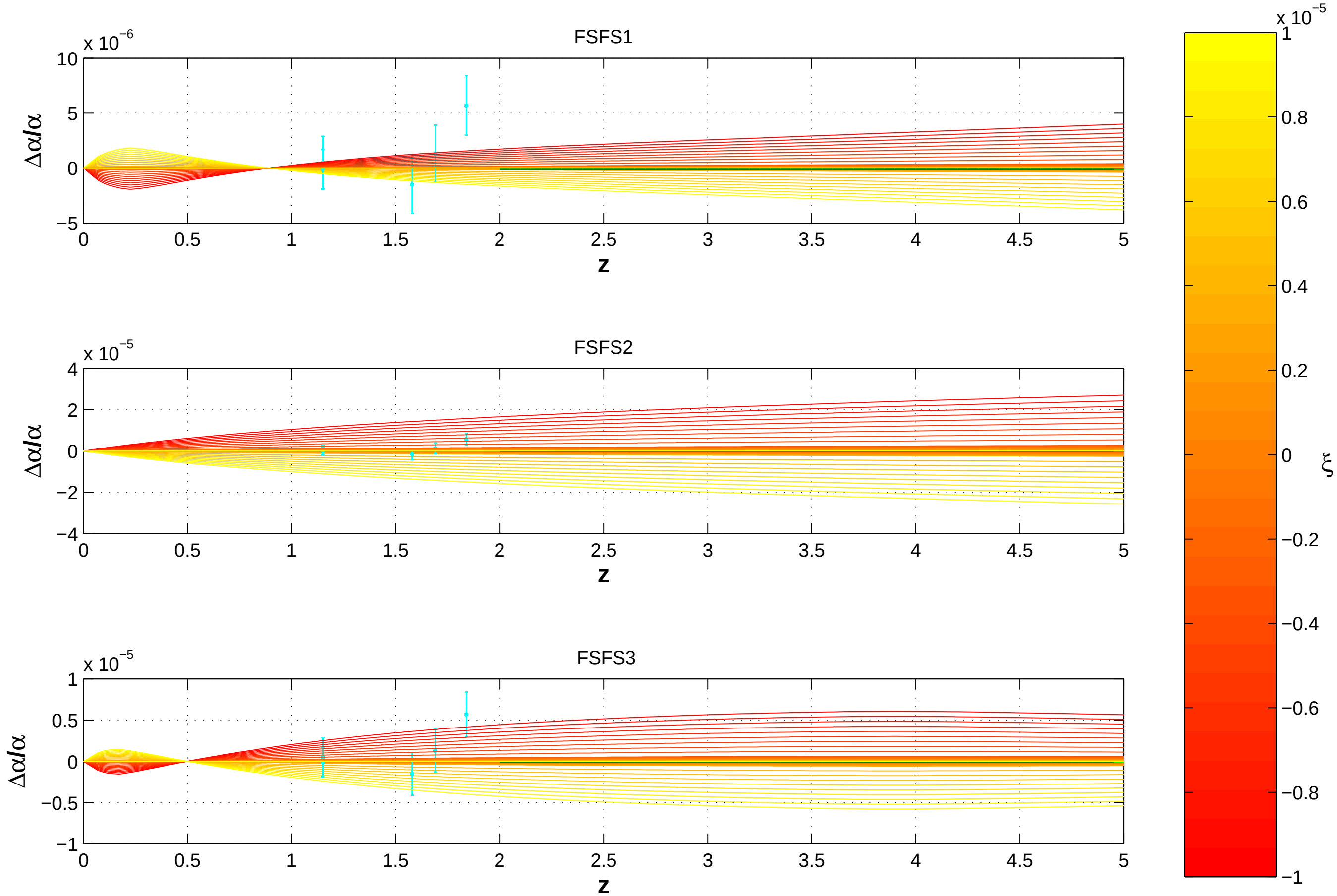

FSFS1
x 10^−6
10
5
0
−5
Δα/α
0
0.5
1
1.5
2
2.5
3
3.5
4
4.5
5
z
FSFS2
x 10^−5
4
2
0
−2
−4
Δα/α
z
FSFS3
x 10^−5
1
0.5
0
−0.5
−1
Δα/α
z
x 10^−5
1
0.8
0.6
0.4
0.2
0
−0.2
−0.4
−0.6
−0.8
−1
ξ

FSFS

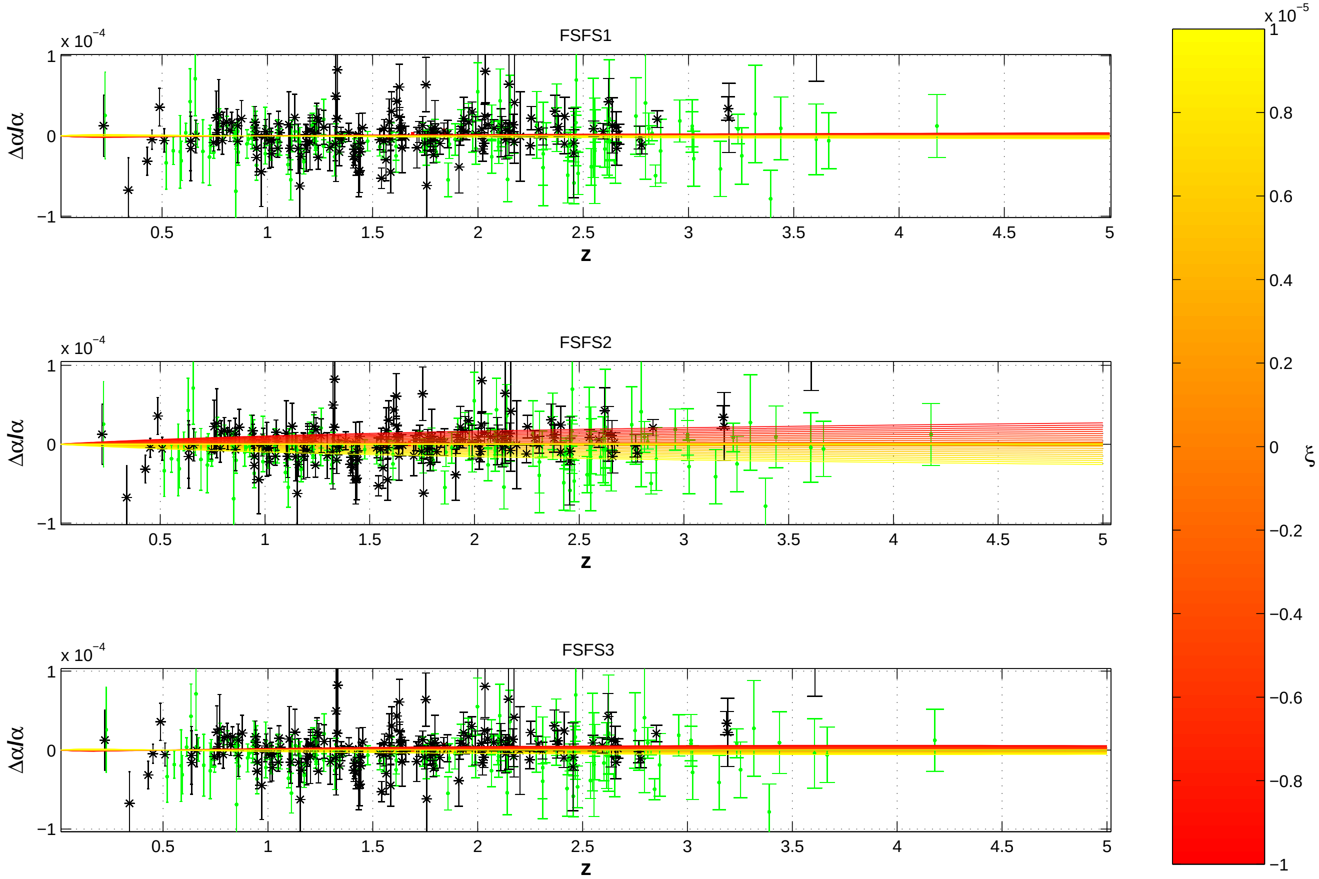

Rosenband bound

In particular at redshift $z = 0$, for which atomic clock measurements provide a very tight limit [1] on the current drift rate of α

$$\left(\frac{\dot{\alpha}}{\alpha}\right)_0 = (-1.6 \pm 2.3) \times 10^{-17} \mathrm{yr}^{-1} . \qquad (28)$$

With the assumptions are making for this class of models we therefore have

$$\left|\frac{\dot{\alpha}}{\alpha}\right|_0 = |\xi| H_0 \sqrt{3\Omega_{\Phi 0} \mid 1 + w_{\Phi 0} \mid} , \qquad (29)$$

where the modulus signs allow for the fact that the models can be at either side of the phantom divide; this leads to the following conservative (three-sigma) bound

$$|\xi| \sqrt{3\Omega_{\Phi 0} \mid 1 + w_{\Phi 0} \mid} < 10^{-6} . \qquad (30)$$

[1] T. Rosenband *et al.*, Science **319**, 1808 (2008).

Rosenband bound

Model	$\Omega_{\Phi 0}$	$w_{\Phi 0}$	$\|\xi\|_{\max} \times 10^7$	$z\|_{\alpha_{max}}$	$\|\Delta\alpha/\alpha\|_{\max} \times 10^6$
SFS1	0.685	-1.064	2.757	1.4	1.47
SFS2	0.685	0.0	0.698	X	X
SFS3	0.685	-0.9171	2.423	2.6	0.80

Table 1: Bounds on the coupling ξ, coming from the atomic clock measurements, for the different models under consideration. Also listed is the maximum allowed variation of α, in the redshift range $0 < z <\leq 5$, when this bound is saturated.

Rosenband bound FSFS

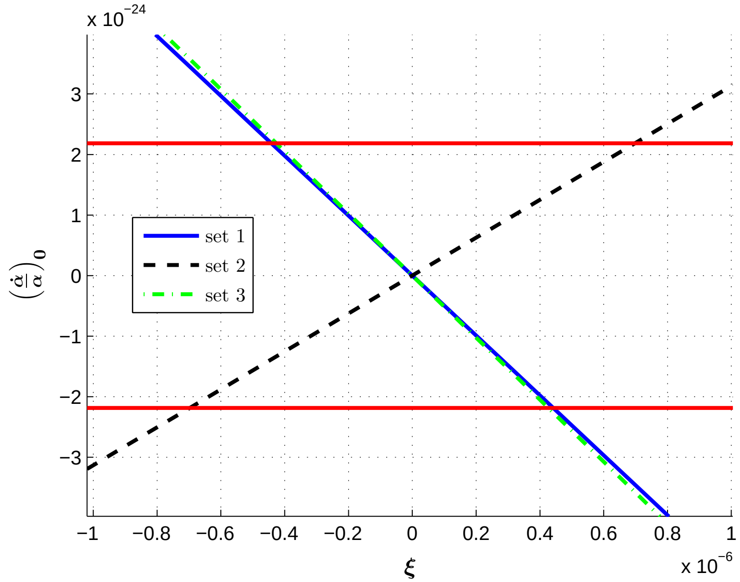

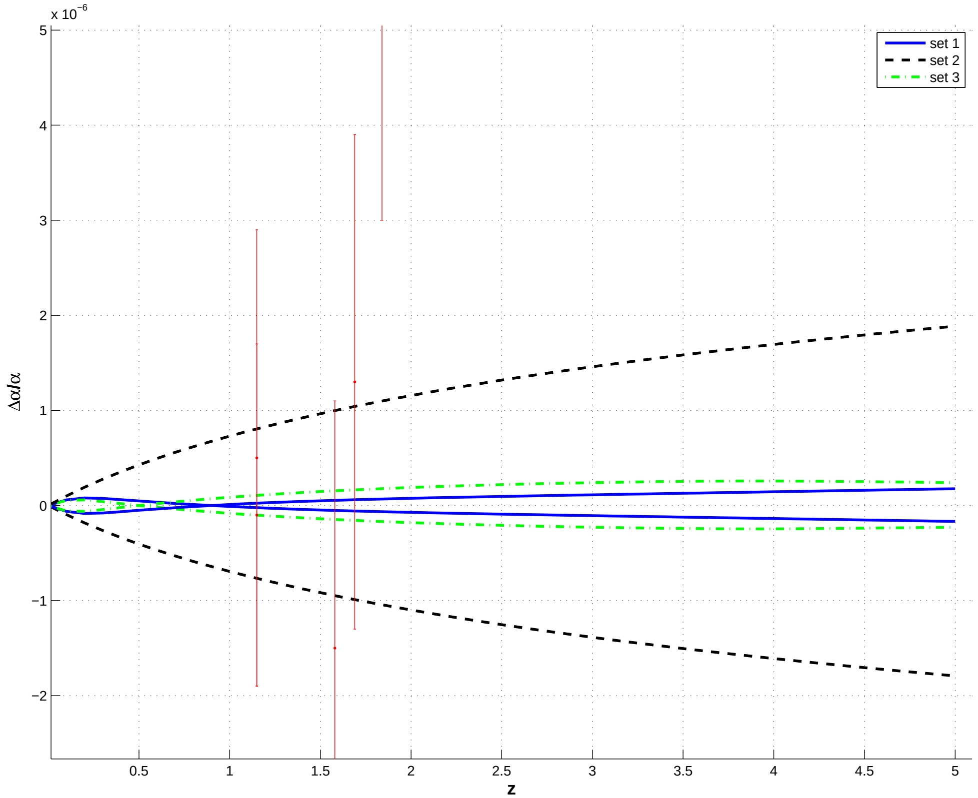

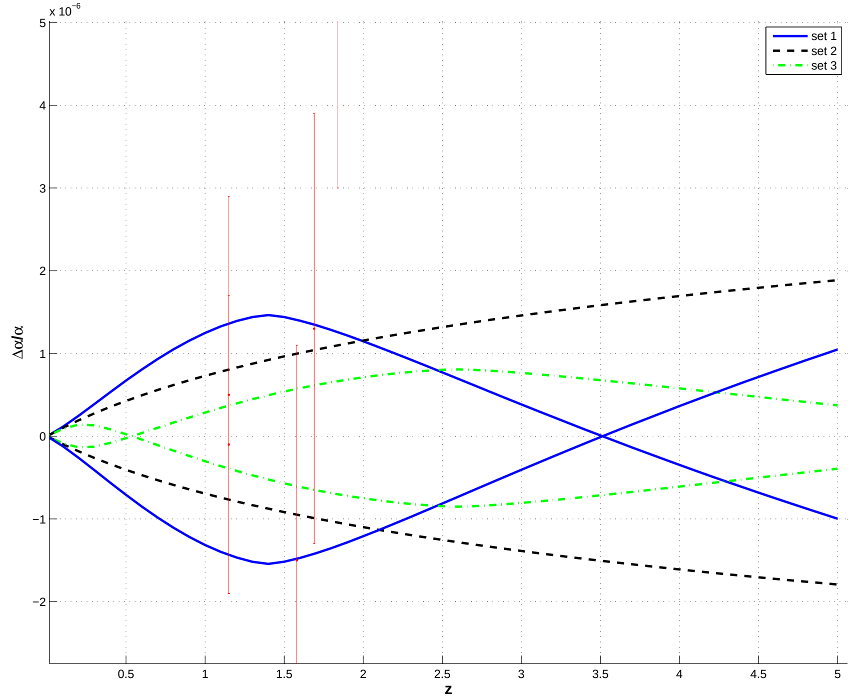

x 10^-6
set 1
set 2
set 3
Δα/α
z

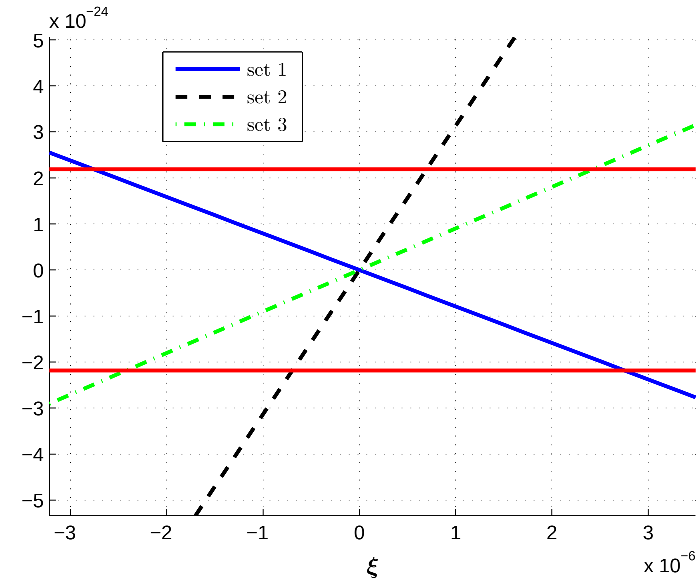

x 10^-24
set 1
set 2
set 3
ξ
x 10^-6

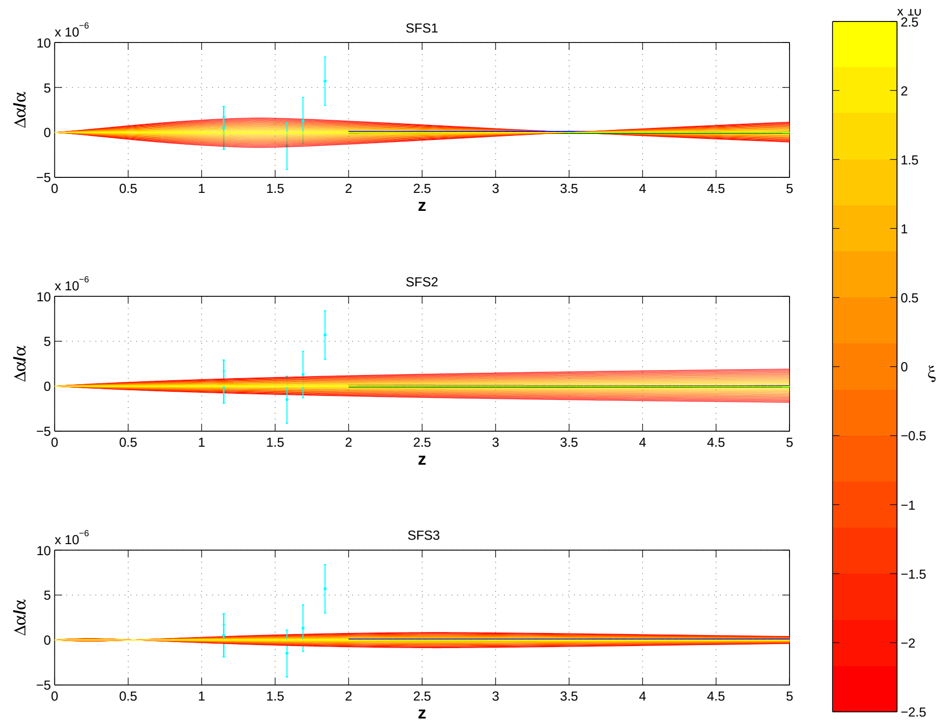

SFS1
SFS2
SFS3
x 10^-6
Δα/α
z
ξ

Conclusions

Outlook

- include some forecasts for ELT-HIRES (high-resolution ultra-stable spectrograph for the E-ELT)
- more stringent constraints onto models parameters from future observations, like: Polarized Radiation and Imaging Spectroscopy (PRISM); Cosmic Origins Explorer (CoRE); Dark Energy Survey (DES); Euclid;
  - possible discrimination between ΛCDM and varying eos models; better constraints onto dark sector perturbations; this gives the motivation for further study of dark sector perturbations;

Thank you!